Agrociencia

INFRARED SPECTROSCOPY ANALYSIS AND CHEMICAL PROPERTIES OF INCEPTISOLS FOR AGRICULTURAL LAND DEVELOPMENT

Rosliana **Eso**[1*], Arman[2]

[1]Halu Oleo University. Department of Geophysics Engineering. Jln HEA Mokodompit, Andonuhu, Kendari City, Indonesia.
[2]Halu Oleo University. Department of Mathematics. Jln HEA Mokodompit, Andonuhu, Kendari City, Indonesia.
* Author for correspondence: rosliana.eso@uho.ac.id

Citation: Eso R, Arman. 2025. Infrared spectroscopy analysis and chemical properties of inceptisols for agricultural land development. **Agrociencia.** https://doi.org/ 10.47163/agrociencia.v59i2.3279

Editor in Chief:
Dr. Fernando C. Gómez Merino

Received: August 05, 2024.
Approved: February 04, 2025.
Published in Agrociencia: March 12, 2025.

ABSTRACT

The purpose of this study was to explore the properties of Inceptisols (Cambisols) to provide fundamental information for agricultural development. The soil type occupies a significant and vital part of the agricultural land, especially in Kendari City, Indonesia. A total of 30 Inceptisol soil samples on limestone parent material were collected from three locations under tree canopy using vertical profiles to identify the physic and chemical properties. The soil mineral was examined by using X-Ray Diffraction (XRD); clay mineral was determined with Fourier Transform Infrared (FTIR) spectroscopy; chemical elements with X-ray Fluorescence (XRF); total nitrogen content with the Kjeldahl method; and soil magnetic properties with a magnetic susceptibility meter. Total nitrogen in the soil was found to range from 0.106% to 0.597%, soil pH ranged from 5.7 to 6.95, and the sand fraction was determined to be the dominant in all profiles, accounting for 60% to 70%. In contrast, oxides of Si, Al, Fe, Mg, Ti, Ca, S, Na, K, P, Mn, Ni, Co, and Cr were identified in the chemical element content. While the increasing trends of Al, Fe, and Mg with depth were largely attributed to limited leaching and slow rates of weathering, the dominant upward trends of Si across all sites indicated significant soil development in the study area. All sites showed upward trends in magnetic susceptibility, indicating the enrichment of magnetic minerals. Although FTIR spectroscopy successfully identified soil minerals at various depths, the diffraction pattern of the topsoil revealed the silicon oxide quartz (SiO_2) phase. At 80 to 200 cm, montmorillonite absorption bands were prominent, while at 0 to 40 cm (topsoil), kaolinite absorption bands dominated. The transformation of montmorillonite into kaolinite in Inceptisol, driven by high mineralization during soil development and restricted leaching and weathering, has a substantial impact on agricultural development and long-term productivity.

Keywords: Inceptisols, Cambisols, FTIR Spectroscopy, Magnetic Susceptibility.

INTRODUCTION

Recent research highlights the importance of understanding the dominant soil development processes and their impact on agricultural utilization (Kartawisastra,

2013). Inceptisols, as defined by the World Reference Base for Soil Resources (Nachtergaele, 2017) and known as Inceptisols in the US soil taxonomy, are particularly significant in soil age sequences. These soils exhibit an intermediate stage of soil development, as evidenced by the development of a cambic horizon but the absence of an argillic horizon (Khresat, 2005).

Inceptisols typically form in environments where soil-forming processes are somewhat inhibited (Dengiz, 2020). By reflecting the initial modifications made to the parent material by soil formation activities, these soils can be studied to provide insight into the early phases of pedogenic processes (Amara *et al*., 2022). Prevalent in mountainous regions, this soil is primarily driven by climatic factors and their altitudinal variations, which influence pedogenic development (Almquist, 2020). In addition to the parent material, climate, terrain, organisms, and time all have an impact on soil formation (Muslim *et al*., 2021). Found in varied habitats, from frigid climates to very warm, humid, and subhumid regions (Stewart, 2019), and ranging from the Arctic to the tropics (Foss *et al*., 1983), the transformation of Inceptisols likely occurs when one or more factors controlling pedogenic processes change.

Inceptisols are widely distributed across Indonesia, particularly in calcareous landforms, and have significant potential for use as agricultural land (Tufaila *et al*., 2016). They develop on old geological materials, which may result from slow pedogenic processes acting upon these soils, active erosion, or gradual weathering (Eso *et al*., 2019). The mean soil texture is clay loam and sandy loam with acidic to slightly acidic soil reactions, with the topsoil having higher organic carbon than the subsoil. Several techniques are used to characterize soil samples, such as physical descriptors (i.e., color, density gradient, particle size, texture, morphology), chemical analysis (i.e., elemental composition, pH, nitrogen content), and magnetic susceptibility properties. Fourier Transform Infrared (FTIR) spectroscopy is used to find valuable data, as forensic soil characterization is a simple, rapid, and non-destructive technical approach that is capable of distinguishing the principal chemical classes of organic matter through the vibrational characteristics of their structural, chemical bonds. Previous studies have successfully described the composition status of different soil horizons (Cox *et al*., 2000; Margenot *et al*., 2019) and determining crystalline silica in industrial dust samples (Ojima, 2003). Magnetic susceptibility is used to express the magnetic mineral content of the soil and to study soil-forming processes (Jordanova, 2016; Maxbauer *et al*., 2016) and soil erosion (Eso *et al*., 2021).

This study aimed to identify the characteristics of Inceptisols (Cambisols) found in calcareous landforms developed from the limestone parent material. Some physical, chemical, and mineral content features can be used to guide soil management and provide balanced fertilizer recommendations. Based on its characteristics, the soil studied can be used for agriculture land, both seasonal and annual crops.

MATERIALS AND METHODS

Site description and sampling method

Soil samples were collected from three locations. A total of 30 samples, taken from depths ranging from 20 to 200 cm across all profiles (each profile comprising 10 samples), were analyzed for physical, magnetic, chemical element, mineral, and organic components. Seasonal crops grown on the existing land included vegetables, while annual crops consisted of oil palm, durian, nutmeg, cloves, and sugarcane. Profiles 1 and 2 were located in the Abeli District, while Profile 3 was situated in the Puwatu District (Figure 1).

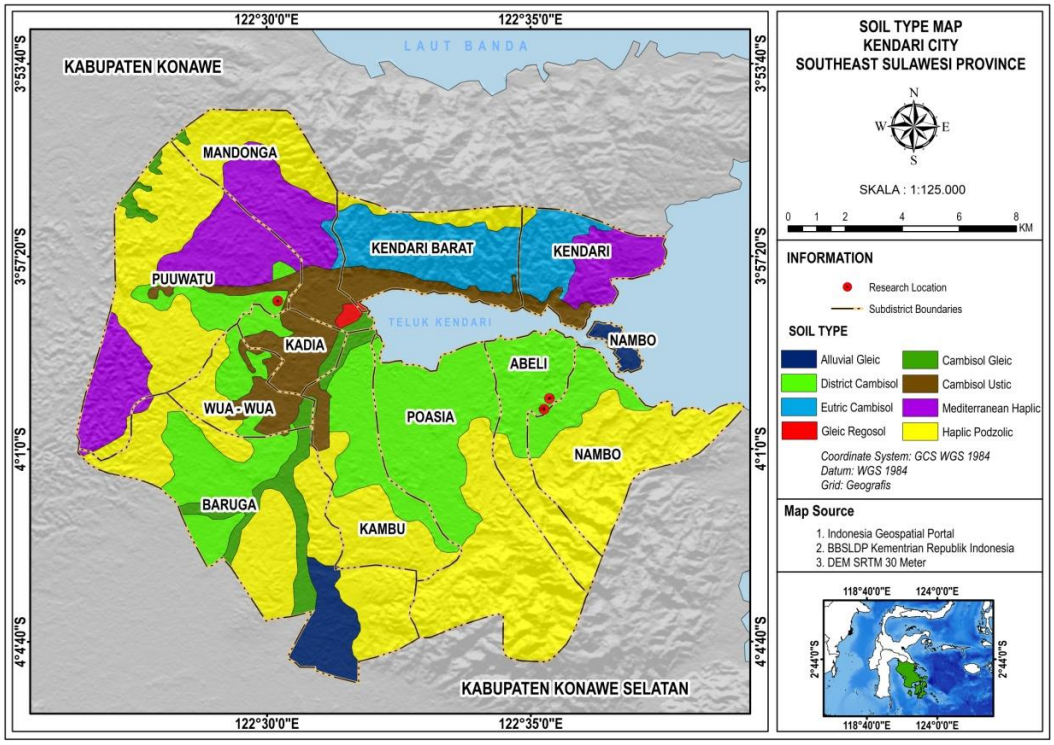

Figure 1. A schematic map of soil types in Kendari City, obtained from the Indonesia Geospatial Portal (http://www.geospatial-indonesia.com), shows the sampling sites in the Abeli and Puwatu districts, marked with rounded red indicators.

Magnetic properties measurement

Analysis of the magnetic properties was conducted at the Earth Physics Laboratory of Halu Oleo University. Magnetic susceptibility was measured at frequencies of 470 Hz and 4700 Hz using a Bartington MS2B susceptibility meter set to a sensitivity of 1.0 (Dearing *et al*., 1996). The mass-specific frequency-dependent susceptibility (c_{FD}) and its percentage (c_{FD} %) were calculated using the following equation

$$\chi_{FD} = \chi_{LF} - \chi_{HF} \quad (1)$$

$$\chi_{FD}\% = \frac{\chi_{LF} - \chi_{HF}}{\chi_{LF}} \times (100)\ \% \quad (2)$$

Here, χ_{LF} and χ_{HF} represent low- and high-frequency susceptibility, respectively. The interpretation of χ_{FD} was used as a proxy to estimate the total concentration of superparamagnetic (SP) grains, following Dearing *et al*. (1996): low χ_{FD} % < 2 %, indicating virtually no SP grains; Medium χ_{FD} % (2–10%) indicating an admixture of SP and coarser non-SP grains or SP grains; High χ_{FD} % (10–14%) indicating predominantly SP grains; and Very high χ_{FD} % (> 14%) indicating rare values or potential contamination.

Soil properties analysis

Major elements were analyzed using X-ray fluorescence (XRF) spectrometry at the Geo Gea Laboratory in Kendari City, Indonesia. Soil samples were air-dried and passed through a 2-mm sieve prior to analysis. Selected soil properties and characteristics were determined according to Soil Survey Staff guidelines (Ditzler and Hempel, 2017), unless stated otherwise. These included pH measurements in water and 1 M KCl using a 1:1 soil-to-solution ratio, and total nitrogen content determined by the Kjeldahl method (Weil and Brady, 2017). Bulk soil fractionation into three particle size fractions (clay, silt, and sand) was performed by wet sieving and sedimentation following Stokes's law (Rossiter, 2011). Reagent blanks were used as quality control samples during the analysis.

Fourier Transform Infrared (FTIR) spectroscopy analysis

In this study, X-ray diffraction (XRD) analysis and Fourier Transform Infrared (FTIR) spectroscopy were employed to characterize the mineral and organic components of soil samples at the Integrated Chemistry Laboratory of Hasanuddin University, South Sulawesi, Indonesia. Samples were crushed into a fine powder using an agate mortar, with grinding time minimized to prevent deformation of the crystal structure and ion exchange. Soil fractions were ground, mixed, and diluted with potassium bromide (0.5–3%), pressed into pellets, and desiccated before analysis. Soil extracts or suspensions were dried onto infrared windows. Since the beam interacts with all areas of the material, the transmission provides a bulk infrared measurement, allowing FTIR spectra of soil minerals and organic components to be obtained

RESULTS AND DISCUSSION

The variation of the magnetic properties of soil

Soil magnetism research is essential for understanding the magnetic characteristics of soil, which plays a key role in explaining plant root development and their function in agricultural productivity. The patterns of magnetic property variation (Figure 2) showed an increasing trend in magnetic susceptibility across all profiles, indicating the enrichment of magnetic minerals. The χLF values for profiles 1, 2, and 3 ranged from 9.59 × 10^{-8} to 36.22 × 10^{-8}, 11 × 10^{-8} to 86.5 × 10^{-8}, and 17.5 × 10^{-8} to 97.85 × 10^{-8} m^3 kg^{-1}, respectively. These values suggest a high concentration of paramagnetic minerals, including olivine, smectite, attapulgite, epidote, and dolomite, which are classified as moderately magnetic (10–100 × 10^{-8} m^3 kg^{-1}) according to soil categories based on magnetic susceptibility (Quijano *et al*., 2014).

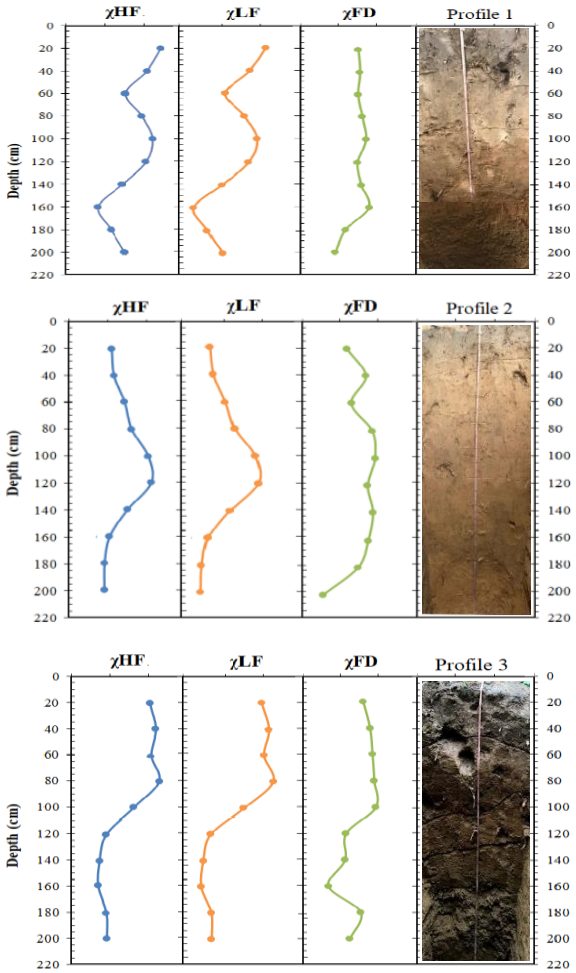

Figure 2. Normalized magnetic susceptibility as a function of depth for profile 1, profile 2 and profile 3.

Profiles 1 and 2 had frequency-dependent susceptibility values ranging from 12.65% to 16.18% and 10.16% to 15.69%, respectively, indicating a high concentration of SP minerals. In contrast, profile 3 exhibited values ranging from 2.04% to 13.97%, with medium values suggesting the presence of SP-enhanced soil minerals (Figure 3)

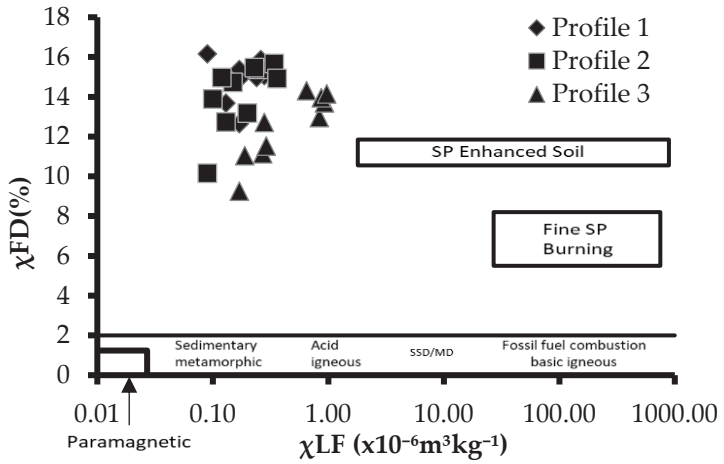

Figure 3. Scattergram of frequency-dependent susceptibility percentage (χFD%) against low-frequency susceptibility (χLF) for three soil vertical profiles, with boxes and labels adapted from Dearing (1999).

Physics and chemical properties of the soil

Inceptisols from these profiles exhibited varying colors depending on land use and mineral content, but were predominantly reddish yellow to dark brown, with hues ranging from 7.5 YR to 10 YR. The value varied from 3 to 7, and chroma ranged from 4 to 8. Soil textures were primarily sand, loamy sand, and sandy loam. The soil reaction (pH) was slightly acidic across all profiles, ranging from 5.5 to 6.5. The mean electrical conductivity was 0.055 dS m^{-1}, with a range from 0.04 to 0.07 dS m^{-1}. The salinity levels were low, and no significant impact on plant growth is expected across all soil profiles (Pooja and Kumar, 2015)

The mechanical composition of all profiles was dominated by the sand fraction (Figure 4), comprising 50–70 % in the different horizons. Silt and clay fractions make a relatively small contribution to the texture and display variations in the lower part of the profile. Although the clay fraction is small in amount, it is relatively enriched in the lower parts of these soils and increases rapidly as it approaches the C horizon. This enrichment is strongly influenced by reduction processes and weak pedogenic clay formation from the primary rock minerals.

Analysis of the chemical elements using the XRF method identified several elements present in all profiles, including oxides of Si, Al, Fe, Mg, Ti, Ca, S, Na, K, P, Mn, Ni, Co, and Cr. These elements exhibit a specific pattern (Figure 5). Si is the most abundant in

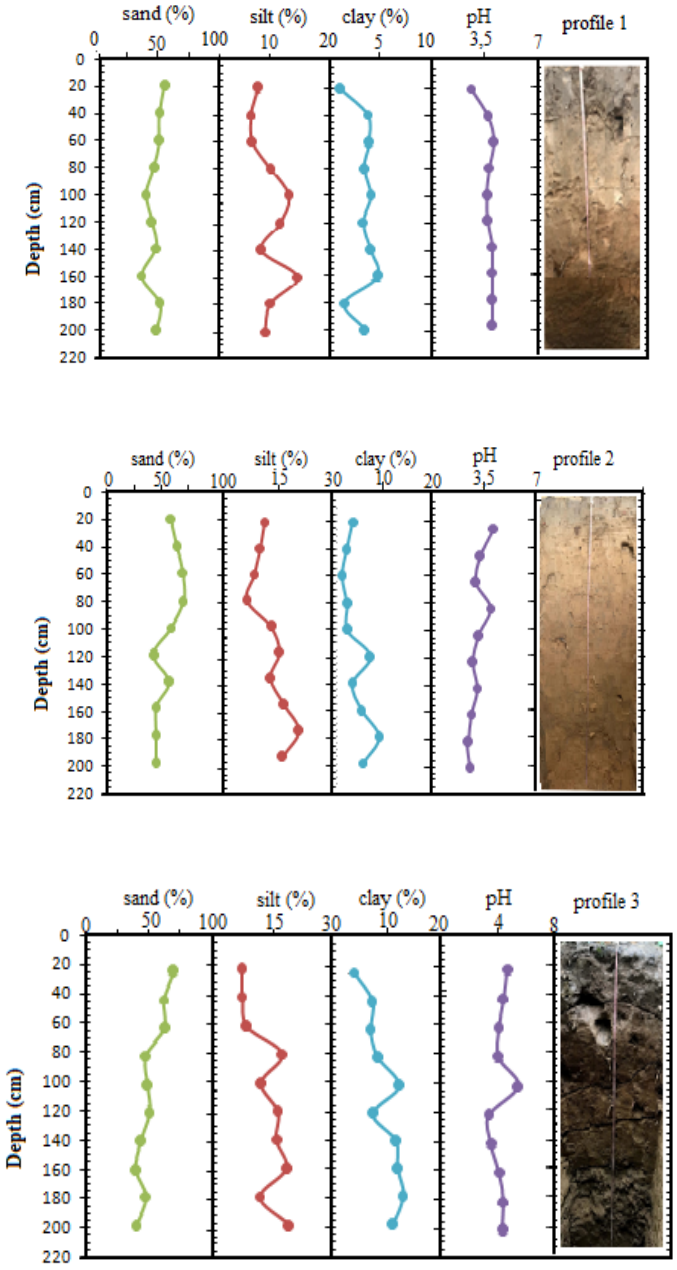

Figure 4. Normalized pH and soil fraction (sand, silt, and clay) as a function of depth for all soil profiles.

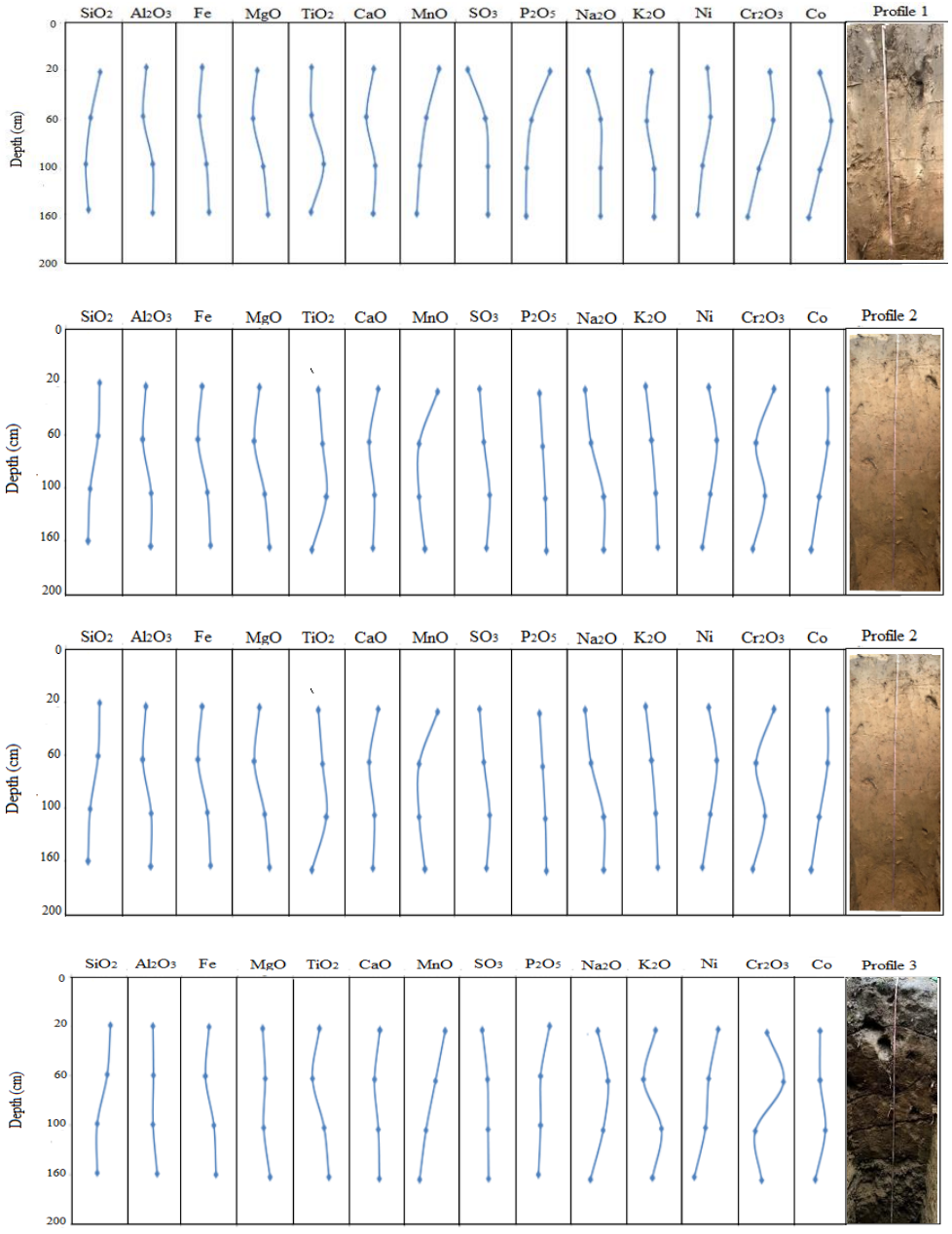

Figure 5. Normalized chemical element content of soil as a function of depth for all soil profiles.

all profiles, ranging from 57.6% to 62.74%, followed by Al (4.1–5.08%), Fe (0.76–1.29%), Mg (0.2–1.15%), Ti (0.198–0.87%), Ca (0.095–0.15%), S (0.04–0.09%), Na (0.01–0.06%), K (0.01–0.043%), P (0.01–0.038%), Mn (0.01–0.038%), and Co, Cr, and Ni, each less than 0.02%. A significant trend was observed when comparing the chemical elements among all soil profiles, showing a unique pattern. Si tends to increase, while Al, Fe, and Mg tend to decrease across all profiles. In contrast, total P and total K, which are critical components of soil fertility, showed a negative trend with depth, indicating higher nutrient availability in the topsoil. Among the various chemical elements found in the soil profiles, the presence of nickel (Ni), chromium (Cr), and cobalt (Co) is particularly significant for soil qualities due to their high magnetic susceptibility and commercial value.

Although associating the variation in magnetic properties with the distribution of chemical elements can be unreliable, the observed patterns may be related to the weathering history of the soils. The results of this comparative characterization demonstrate some distinct differences between the magnetic characteristics and chemical elements in the soil profile. The observed differences are consistent with the hypothesis that the high-Fe soil has experienced more intense weathering resulting from either the higher Fe concentration, the lower magnetic properties, or both. Further work is needed to explain the observed difference between the high-Fe and control soil and to identify specific mechanisms by which altered weathering conditions determine weathering rates.

Total nitrogen and chemical mineral composition of soil

The average total nitrogen of soil ranged from 0.21 to 0.59 % for profile 1, from 0.1 to 0.48 % for profile 2, and from 0.1 to 0.39 % for profile 3 (Figure 6). Total nitrogen levels on topsoil are increasing, meeting the medium criteria for profiles 1 and 2 and the low criteria for profile 3.

The diffraction pattern of the topsoil from all profiles (Figure 7) revealed a 100% silicon oxide (SiO_2) phase with a trigonal (hexagonal axis) crystal system. The peak positions

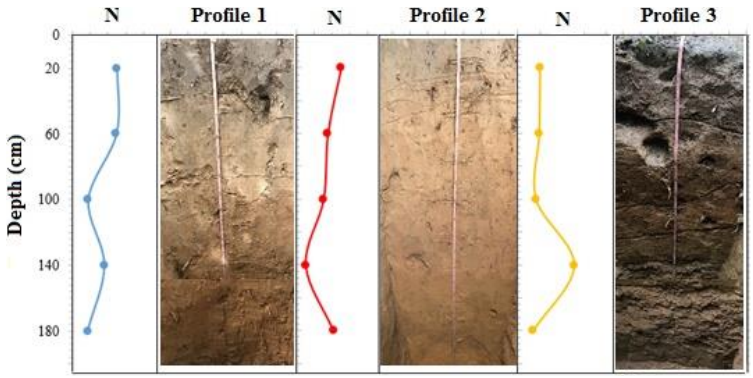

Figure 6. Total nitrogen content in vertical layer of soil horizon for all profiles.

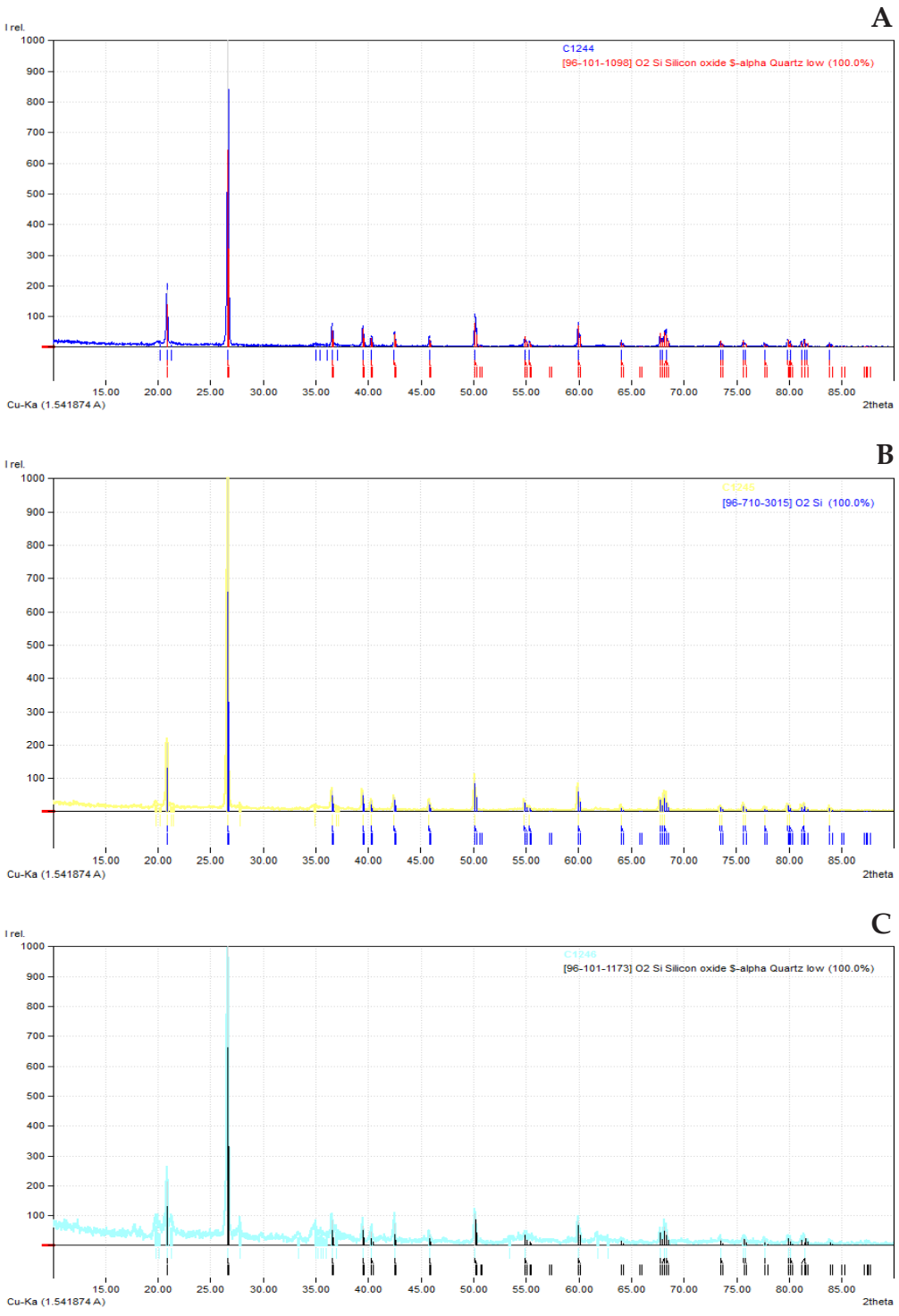

Figure 7. The diffraction pattern of the topsoil: Profile 1 (A), Profile 2 (B), and Profile 3 (C).

in the 2θ angle correspond to low quartz minerals, with the three highest peaks at angles 26.64°, 20.86°, and 50.14°.

FTIR variation

Soil evaluation using FTIR spectroscopy with an infrared spectrum (400–4000 cm^{-1}) (Figure 8) revealed the nature of the frequency groups at three soil sites, showing fluctuations with depth (i.e., 20, 40, 80, 120, 160, and 200 cm, respectively), which were generally governed by fundamental vibrations.

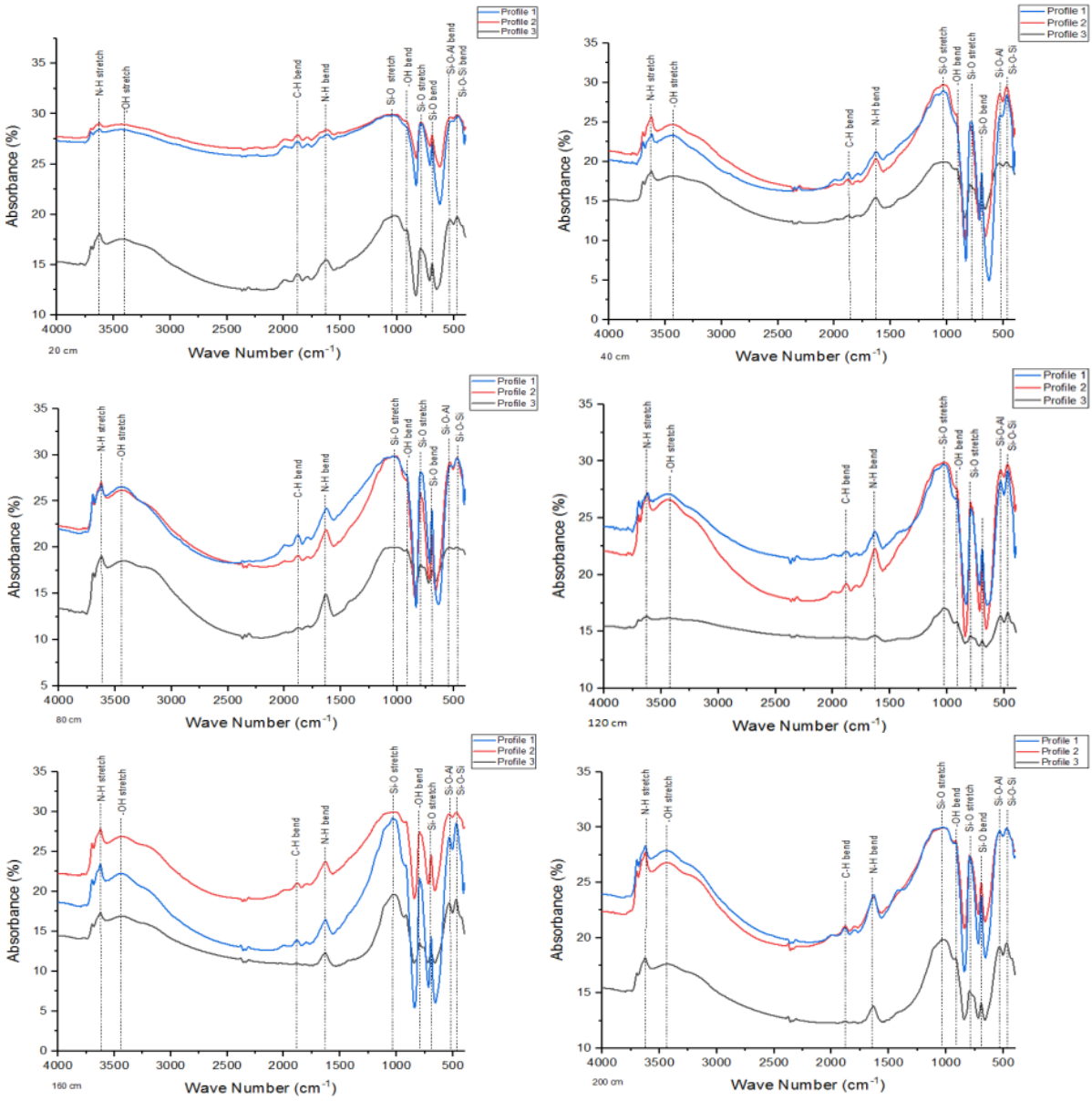

Figure 8. Comparison of Fourier Transform Infrared (FTIR) spectroscopy spectra of topsoil from Abeli District (left) and Puwatu District (right).

Absorbance bands corresponding to organic functional groups indicate an index of soil organic matter (SOM) humification at all profiles, which is higher in topsoil than in subsoil, including alcohols (O-H) stretching in strong board (3420–3440 cm^{-1}), aliphatic primary amines (N-H) (3697–3620 cm^{-1}), amine and cyclic alkenes (1665–1630 cm^{-1}) due to N-H bending, C=C stretching vibration, and aliphatic C-H bending at 1872 cm^{-1}. However, overlapping low absorbance intensity of organic functional groups and dominant absorbance of mineral components, particularly Si-O stretching, occur in the region 1100–800 cm^{-1}, making interpretation difficult on this band.

Soil mineral absorbance bands corresponding to phyllosilicates groups, including hydroxyl (O-H) stretching and bending, occur at 3700–3620 and 920–916 cm^{-1}. Silicate Si-O asymmetric stretching occur at 1090–1030 cm^{-1}, Si-O symmetric stretching at 795–790 cm^{-1}, and Si-O bending at 695–690 cm^{-1}. Specific absorption of the fingerprint region was sensitive enough to distinguish Si-O-Al and Si-O-Si bending, allowing for the identification of the phyllosilicate structural class (Krivoshein *et al*., 2020).

Layer silicates are made up of Al in octahedral coordination with O bonded to one (1:1) or two (2:1) sheets of Si in tetrahedral coordination with oxygen. Structural characterization and phylosilicate identification are based on the absorbance of mineral structural units. The 1:1-layer silicates (Figure 8) show two or more OH stretching bands at depths of 20 and 40 cm across all profiles, whereas the 2:1-layer silicates exhibit a single OH stretching band (3700–3620 cm^{-1}) at depths of 80, 120, 160, and 200 cm, which is attributed to OH coordinated with octahedral cations

IR spectroscopy in the range of O-H stretching vibrations is one of the most accurate methods for identifying phyllosilicates in polymineral mixtures. The primary absorption band spectra from topsoil to 40 cm depth across all profiles show a single OH stretching vibration in the hydroxyl group region (3700–3400 cm^{-1}). A single peak at 3694 and 3620 cm^{-1} can be classified as a 2:1 layer of kaolinite, while a broad absorbance in the Si-O stretching region (1120–950 cm^{-1}) shows peaks at 1114, 1032, 1010, and 936 cm^{-1}

Furthermore, in the 80 to 200 cm depth range, peaks at 3629 and 3620 cm^{-1} are classified as a 1:1 layer silicate, with two OH stretching bands and two broad Si-O stretching absorbances at the 1044 and 918 cm^{-1} peaks. Overall, based on IR spectrum band absorption, the soil mineral type from 80 to 200 cm depth resembles the montmorillonite absorption band, while the topsoil to 40 cm depth corresponds to the kaolinite absorption band (Ojima, 2003).

High levels of Al, Fe, and Mg in the soil, with these patterns increasing with depth (Figure 8), indicated Al_2OH vibration (3620 and 916 cm^{-1}), FeAlOH (890–910 cm^{-1}), and MgAlOH (850 cm^{-1}) in montmorillonite (Madari *et al*., 2006). In contrast, the 1:1 layer silicate attributed to kaolinite is expressed in terms of Si-O absorbance at 1120–950 cm^{-1}. It appears that, using an FTIR analysis approach, variations in clay minerals from montmorillonite to kaolinite in the topsoil throughout the profiles could be explored.

Micro-ATR spectroscopy was used to study the effect of clay swelling on the misorientation and physical breakdown of montmorillonite platelets (Du and Zhou, 2011). The shift from montmorillonite to kaolinite in topsoil affects soil properties, water dynamics, and fertility, all of which are critical for agricultural development. Sustainable land management practices must adapt to these changes, such as adding organic matter to soils (Wilding and Drees, 1983), implementing crop rotation to maintain nutrient-holding capacity, developing irrigation strategies, and selecting crops suited to ensure optimal yield productivity

The abundance of magnetic minerals with upward trends from the bottom of the rock strata supports long-term pedogenic processes (Maxbauer *et al*., 2017). The χ_{LF} values at all profiles ranged from 9.59×10^{-8} to 97.85×10^{-8} $m^3\ kg^{-1}$, indicating a high concentration of paramagnetic minerals such as olivine, smectite, attapulgite, epidote, and dolomite. The average frequency-dependent susceptibility values in all profiles ranged from 12.65% to 16.18%, indicating that bulk superparamagnetic minerals strongly influence weathering through chemical, physical, and environmental factors. The abundance of Si, followed by Al, Ca, Fe, Ti, Na, S, and Mn, can be linked to the weathering history of the soils. Slow weathering rates present substantial challenges to agricultural development due to slow nutrient replenishment and poor water retention.

Total nitrogen values in all sample sites were higher in the topsoil than in the subsoil. It is unclear whether the high nitrogen values in all profiles are driven by anthropogenic or pedogenic processes (de Vries and Posch, 2011). Because nitrate ions and clay-humus particle surfaces are negatively charged, NO_3^- is easily leached with drainage water unless it is taken up by organisms or denitrified. The strong affinity of H^+ ions for negatively charged surfaces can lead to the displacement of cations such as Ca^{2+}, Mg^{2+}, and K^+ from particle exchange surfaces (Margenot *et al*., 2019). The vibrations of relevant atomic groupings vary in frequency to an extent that corresponds to IR bands associated with mineral identification in the sample material

The diffraction pattern of topsoil from the three profiles (Figure 7) was identified as quartz-low (SiO_2), indicating the need to investigate their interference with minerals in the main absorption band (Dewi *et al*., 2018). As a result, Inceptisol topsoil had the highest mineral essential for crop formation as a result of physical change. Clay minerals, such as montmorillonite (high fertility), must be transformed into kaolinite (low fertility) using natural resource management and sustainable farming technologies.

CONCLUSIONS

This study examined the chemical and magnetic properties of Inceptisol soil under tree canopies, along with Fourier Transform Infrared (FTIR) spectroscopy analysis. The analysis revealed a range of chemical element contents, each exhibiting a distinct pattern. The average total nitrogen content of the soil ranged from 0.14% to 0.51%, with values increasing sequentially from the underlying bedrock to the topsoil. The

variation in magnetic susceptibility across all sites showed an upward trend, indicating the enrichment of magnetic minerals and, thus, the prolonged influence of pedogenic processes

IR spectrum band absorption corresponding to organic functional groups serve as an index of soil organic matter humification across all profiles, including alcohol and aliphatic primary amine stretches, as well as amines and cyclic alkenes. Understanding the swelling and physical breakdown of montmorillonite platelets requires collaborative efforts to implement sustainable soil management practices aimed at maintaining soil health and ensuring long-term productivity. Mineral modification using additives can enhance the properties of montmorillonite or stabilize kaolinite soils, thereby supporting long-term agricultural productivity and improved land use.

REFERENCES

Almquist VW. 2020. Integrating complex soil dynamics using the non-equilibrium effective temperature. Frontiers in Earth Science 8 (1). https://doi.org/10.3389/feart.2020.00001

Amara DMK, Sawyerr PA, Saidu DH, Vonu OS, Musa RM, Mboma JCA, Kamanda PJ, Sannoh MA. 2022. Studies on the genesis of soils in Jong River basin in the northern province of Sierra Leone. Scientific Research Publising. Open Journal of Geology 12 (3): 273–293. https://doi.org/10.4236/ojg.2022.123015

Cox RJ, Peterson HL, Young J, Cusik C, Espinoza EO. 2000. The forensic analysis of soil organic by FTIR. Forensic Science International 108 (2): 107–116. https://doi.org/10.1016/s0379-0738(99)00203-0

de Vries, Posch WM. 2011. Modelling the impact of nitrogen deposition, climate change and nutrient limitations on tree carbon sequestration in Europe for the period 1900-2050. Environmental Pollution 159 (10): 2289–2299. https://doi.org/10.1016/j.envpol.2010.11.023

Dearing JA, Dann RJL, Hay K, Lees J A, Loveland PJ, Maher BA, Grady K. 1996. Frequency-dependent susceptibility measurements of environmental materials. Geophysical Journal International 124 (1): 228–240. https://doi.org/10.1111/j.1365-246X.1996.tb06366.x

Dengiz O. 2020. Soil quality index for paddy fields based on standard scoring functions and weight allocation method. Archives of Agronomy and Soil Science 66 (3): 301–315. https://doi.org/10.1080/03650340.2019.1610880

Dewi R, Agusnar H, Alfian Z, Tamrin. 2018. Characterization of technical kaolin using XRF, SEM, XRD, FTIR and its potentials as industrial raw materials. Journal of Physics: Conference Series 1116 (4): 8–14. https://doi.org/10.1088/1742-6596/1116/4/042010

Du C, Zhou J. 2011. Application of infrared photoacoustic spectroscopy in soil analysis. Applied Spectroscopy Reviews 46 (5): 37–41.
https://doi.org/10.1080/05704928.2011.570837

Eso R, Safiuddin LO, Bijaksana S, Ngkoimani LO, Agustine E, Tamuntuan G, Ardin. 2019. Patterns of variation magnetic properties and chemical elements of soil profile in landslide area of South East Sulawesi Indonesia. IOP Conference Series: Earth and Environmental Science 311 (1): 012008. https://doi.org/10.1088/1755-1315/311/1/012008

Eso R, Tufaila M, Safiuddin LO, Syaf H. 2021. Magnetic properties and nitrogen content of soil exposed by lightning. JP Journal of Heat and Mass Transfer 23 (2): 341–357. https://doi.org/10.17654/HM023020341

Foss JE, Moormann FR, Rieger S. 1983. Inceptisols. *In* Wilding LP, Smeck NE, Hall GF (Eds.), Developments in Soil Science. Elsevier: Amsterdam, Netherlands; pp. 355-381. https://doi.org/10.1016/S0166-2481(08)70621-4.

Jordanova N. 2017. Soil magnetism: Applications in pedology, environmental science and agriculture. Academic Press: San Diego, CA, USA. https://doi.org/10.1016/B978-0-12-809239-2.01001-9

Kartawisastra S. 2013. Development of soil classification and soil resource inventory method in Indonesia. *In* Proceeding of International Workshop on Globalsoilmap.net Oceania Node. Bogor, Indonesia.

Khresat SA. 2005. Formation and properties of Inceptisols (Cambisols) of major agricultural rainfed areas in Jordan. Archives of Agronomy and Soil Science 51 (1): 15–23. https://doi.org/10.1080/03650340400026545

Krivoshein PK, Volkov DS, Rogova OB, Proskurnin MA. 2020. FTIR photoacoustic spectroscopy for identification and assessment of soil components: Chernozems and their size fractions. Photoacoustics 18: 100162. https://doi.org/10.1016/j.pacs.2020.100162

Madari BE, Reeves JB, Machado PLOA, Guimarães CM, Torres E, Mccarty GW. 2006. Mid- and near-infrared spectroscopic assessment of soil compositional parameters and structural indices in two Ferralsols. Geoderma 136 (1–2): 245–259. https://doi.org/10.1016/j.geoderma.2006.03.026

Margenot AJ, Parikh SJ, Calderón FJ. 2019. Improving infrared spectroscopy characterization of soil organic matter with spectral subtractions. Journal of Visualized Experiments 143. https://doi.org/10.3791/57464

Maxbauer DP, Feinberg JM, Fox DL. 2016. Magnetic mineral assemblages in soils and paleosols as the basis for paleoprecipitation proxies: A review of magnetic methods and challenges. Earth-Science Reviews 155: 28–48. https://doi.org/10.1016/j.earscirev.2016.01.014

Maxbauer DP, Feinberg JM, Fox DL, Nater EA. 2017. Response of pedogenic magnetite to changing vegetation in soils developed under uniform climate, topography, and parent material. Scientific Reports 7 (1): 17575. https://doi.org/10.1038/s41598-017-17722-2

Muslim RQ, Kricella P, Pratamaningsih MM, Purwanto S, Suryani E, Ritung S. 2021. Characteristics of Inceptisols derived from basaltic andesite from several locations in volcanic landform. Sains Tanah 17 (2): 115–121. https://doi.org/10.20961/stjssa.v17i2.38221

Nachtergaele FO. 2017. Classification systems: FAO. Earth Systems and Environmental Sciences. Academic Press: San Diego, CA, USA. https://doi.org/10.1016/B978-0-12-409548-9.10520-2

Ojima J. 2003. Determining of crystalline silica in respirable dust samples by Infrared Spectrophotometry in the presence of interferences. Journal of Occupational Health 45 (2): 94–103. https://doi.org/10.1539/joh.45.94

Pooja S, Kumar R. 2015. Soil salinity: A serious environmental issue and plant growth promoting bacteria as one of the tools for its alleviation. Saudi Journal of Biological science 22 (2): 123–131. https://doi.org/10.1016/j.sjbs.2014.12.001

Quijano L, Chaparro MAE, Marié DC, Gaspar L, Navas A. 2014. Relevant magnetic and soil parameters as potential indicators of soil conservation status of Mediterranean agroecosystems. Geophysical Journal International 198 (3): 1805–1817. https://doi.org/10.1093/gji/ggu239

Rossiter DG. 2011. Manual of methods for soil and land evaluation. Soil Science Society of America Journal 5 (3): 1174. https://doi.org/10.2136/sssaj2011.0001br

Stewart RL. 2019. Soil and climate. CRC Press: Boca Raton, FL, USA. 400 p.

Tufaila M, Safiuddin LO, Eso R, Kasmiati S, Syaf H, Nur-Ramadhan LOA, Ardin. 2016. Variation of chemical elements and their associations in laterite soil profile. Journal of Tropical Soils 20 (2): 111–118. https://doi.org/10.5400/jts.2015.v20i2.111-118

Ditzler CA, Hempel J. 2017. Soil taxonomy and soil classification. *In* International Encyclopedia of Geography. Wiley: Hoboken, NJ, USA. https://doi.org/10.1002/9781118786352.wbieg0347

Weil RR, Brady NC. 2017. The nature and properties of soil (15th edition). Pearson Education: Hoboken, NJ, USA. 1104 p.

Wilding LP, Drees LR. 1983. Spatial variability and pedology. Wilding LP, Smeck NE, Hall GF. (eds), Developments in Soil Science (Volume 11). Elsevier: Amsterdam, Netherlands, pp: 83–116. https://doi.org/10.1016/S0166-2481(08)70599-3